JOURNAL OF AIRCRAFT
Vol. 34, No. 3, May–June 1997

Inverse Design Method for Transonic Multiple Wing Systems Using Integral Equations

Kisa Matsushima*
Fujitsu Ltd., Chiba 261, Japan
and
Susumu Takanashi† and Toshiyuki Iwamiya‡
National Aerospace Laboratory, Tokyo 182, Japan

An inverse design method that treats multiple wings (or multicomponents of a wing) is proposed and examined. The method takes into consideration the mutual interaction among wings. It designs the section shapes of wings that realize a specified surface pressure distribution. It can be applied to two- and three-dimensional aerodynamic design problems in various degrees of a flowfield, potential flow, inviscid and viscous flow, subsonic and transonic flow. The primary idea is the extension of an integral equation method. An inverse problem is reformulated in terms of integral equations that express the relation of pressure differences to geometrical changes of wing sections for a multiple wing system. Most of the integral calculation is done analytically and the equations are solved numerically by introducing piecewise function approximation. This method works well on several preliminary design problems in transonic and high subsonic flows. From the practical point of view, it is promising for complicated aerodynamic design.

Nomenclature

$Cp(x, y)$	=	surface pressure distribution
c_k	=	z location of the mean plane of wing-k
$f(x, y)$	=	shape function of wing section contours
$I(k), J(k) + 1$	=	number of panels in x and y directions of wing-k
K	=	$(\gamma + 1)M_\infty^2$
M_∞	=	freestream Mach number
x, y, z	=	Cartesian coordinates of a flowfield
β	=	parameter for Prandtl–Glauert transformation of a coordinate system, $(1 - M_\infty^2)^{1/2}$
γ	=	ratio of specific heats
$\Delta Cp(x, y)$	=	difference between target Cp and original one
$\Delta f(x, y)$	=	correction of $f(x, y)$
$\Delta\phi(x, y, z)$	=	change of $\phi(x, y, z)$
ξ, η, ζ	=	coordinate system for Green's function integration
$\phi(x, y, z)$	=	perturbation velocity potential
$\chi(x, y, z)$	=	variation of nonlinear term of the transonic small disturbance equation by change of $\phi(x, y, z)$, $\frac{1}{2}\{[\phi_x + (\Delta\phi)_x]^2 - \phi_x^2\}$

Subscripts

k	=	quantity concerning wing-k
$+$	=	quantity on an upper wing surface
$-$	=	quantity on a lower wing surface

Presented as Paper 96-2465 at the AIAA 14th Applied Aerodynamics Conference, New Orleans, LA, June 17–20, 1996; received Aug. 29, 1996; revision received Jan. 8, 1997; accepted for publication Jan. 9, 1997.

*Senior Engineer, HPC Systems Engineering Division, Makuhari Systems Laboratory, Nakase 1-9-3, Mihama-ku, Chiba-shi. Member AIAA.

†Principal Scientist, Computational Aerodynamics Laboratory, Aircraft Aerodynamics Division (Deceased).

‡Principal Scientist, Applied Mathematics Laboratory, Computational Sciences Division, Jindaiji-higashi-machi 7-44-1, chofu-shi.

I. Introduction

AUTOMATIC aerodynamic design of aircraft components has become attractive as one of the many applications of computational fluid dynamics (CFD). For the aerodynamic shape design, an inverse method is considered to take an important integral part, because a designer can control aerodynamic characteristics over aircraft components directly and precisely by prescribing the pressure distribution at their surfaces. Numerous methods to solve an inverse problem have been devised.[1,2] Some of the inverse design methods, such as the constrained direct iterative surface curvature method (CDISC),[3] have steadily made progress and been applied to practical problems. An integro-differential equation method for transonic wing design formulated and developed by one of the authors[4] is regarded to be one of the fastest and most versatile inverse design algorithms.[2] It has been widely applied to aerodynamic design problems.[5–10] Most formulations of an inverse problem have been aimed to design a single component in a flowfield. On the other hand, remarkable progress in flow analysis methods and computers enabled us to simulate complicated flowfields of multiple wings and aircraft's components. A design method that can treat multiple wings (or components) has become practically useful for aerodynamic design. Ormsbee and Chen,[11] Narramore and Beaty,[12] and Shigemi[13] pioneered the inverse design of multielement airfoils in incompressible potential flow. No subsequent developments of the inverse design of multiple components have been published as far as the authors know; whereas several design methods using a numerical optimization algorithm have been applied to the design of multielement airfoils.[14] In this paper, an inverse design problem for multiple wings in a transonic flowfield is formulated. The formulation is the extension of Takanashi's method.[4] The new formulation takes into consideration wings' mutual interactions to design wing section shapes. The results of design problems demonstrate the feasibility of the new formulation.

II. Formulation

To determine section shapes of plural wings in a flowfield simultaneously, an integral equation system is derived from the

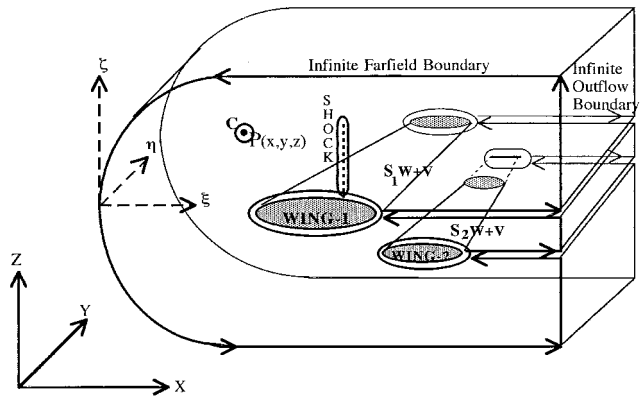

Fig. 1 Coordinate system for formulation.

following three equations of fluid dynamics. The concept of the formulation is to build the mathematical model that relates geometrical correction to pressure differences. A flowfield where k_{max} wings (wing-1, wing-2, and wing-k_{max}) exist is approximated by using the thin wing theory. The coordinate system is indicated in Fig. 1, where x axis is streamwise, y axis is spanwise, and z axis is in the thickness direction of wings. We are going to treat transonic and subsonic flowfields. The freestream Mach number is less than 1, and the freestream velocity is normalized as (1, 0, 0). Then the flowfield is described by the transonic small disturbance equation:

$$(1 - M_\infty^2)\bar{\phi}_{\bar{x}\bar{x}} + \bar{\phi}_{\bar{y}\bar{y}} + \bar{\phi}_{\bar{z}\bar{z}} = (\gamma + 1)M_\infty^2 \frac{\partial}{\partial \bar{x}}\left(\frac{1}{2}\bar{\phi}_{\bar{x}}^2\right) \quad (1)$$

The pressure coefficients on each wing surface are expressed as

$$Cp_{k\pm}(\bar{x}, \bar{y}) = -2\bar{\phi}_{\bar{x}}(\bar{x}, \bar{y}, c_k \pm 0) \qquad (k = 1, 2, \ldots, k_{max}) \quad (2)$$

The flow tangency condition on each wing can be written as

$$\bar{\phi}_{\bar{z}}(\bar{x}, \bar{y}, c_k \pm 0) = \frac{\partial}{\partial \bar{x}}\bar{f}_{k\pm}(\bar{x}, \bar{y}) \qquad (k = 1, 2, \ldots, k_{max}) \quad (3)$$

The notations, $+0$ and -0, are the upper and lower surface of each wing, respectively.

Using the Plandtl–Glauert transformation such as

$$x = \bar{x}, \qquad y = \beta\bar{y}, \qquad z = \beta\bar{z}$$

$$\phi(x,y,z) = (K/\beta^2)\bar{\phi}(\bar{x}, \bar{y}, \bar{z}), \qquad f_\pm(x, y) = (K/\beta^3)\bar{f}_\pm(\bar{x}, \bar{y}),$$

Equations (1–3) yield to Eqs. (4–6), respectively:

$$\phi_{xx} + \phi_{yy} + \phi_{zz} = \frac{\partial}{\partial x}\left(\frac{1}{2}\phi_x^2\right) \quad (4)$$

$$Cp_{k\pm}\left(x, \frac{y}{\beta}\right) = -2\frac{\beta^2}{K}\phi_x(x, y, c_k \pm 0) \quad (k = 1, 2, \ldots, k_{max}) \quad (5)$$

$$\phi_z(x, y, c_k \pm 0) = \frac{\partial}{\partial x} f_{k\pm}(x, y) \qquad (k = 1, 2, \ldots, k_{max}) \quad (6)$$

Let us think of two flowfields: the perturbation velocity potential of an arbitrary flowfield is denoted by $\phi'(x, y, z)$ and that of the other flowfield is denoted by $\phi^T(x, y, z) = \Delta\phi + \phi'(x, y, z)$. According to Eq. (4), $\Delta\phi$ is expressed as

$$(\Delta\phi)_{xx} + (\Delta\phi)_{yy} + (\Delta\phi)_{zz} = \frac{\partial}{\partial x}\left\{\frac{1}{2}[(\phi')_x + (\Delta\phi)_x]^2 - \frac{1}{2}(\phi')_x^2\right\} \quad (7)$$

The pressure distribution on each wing surface corresponding to ϕ^I is Cp_k^I. That corresponding to ϕ^T is Cp_k^T. The difference, $\Delta Cp_k = Cp_k^T - Cp_k^I$ ($k = 1, \ldots, k_{max}$), is related to the change in the x velocity on each wing surface as

$$\Delta Cp_{k\pm}(x, y/\beta) = -2(\beta^2/K)[\Delta\phi(x, y, c_k \pm 0)]_x \qquad (k = 1, 2, \ldots, k_{max}) \quad (8)$$

The geometric correction of each wing $\Delta f_k(x, y)$, $k = 1, 2, \ldots, k_{max}$, is related to the change in the z velocity on each wing surface as

$$[\Delta\phi(x, y, c_k \pm 0)]_z = \frac{\partial}{\partial x}[\Delta f_{k\pm}(x, y)] \quad (k = 1, 2, \ldots, k_{max}) \quad (9)$$

Applying Green's theorem to Eq. (7), performing integration by parts, and using the divergence theorem on the volume integral,[15] we obtain

$$\begin{aligned}\Delta\phi(x, y, z) = &-\frac{1}{4\pi}\sum_{k=1}^{k_{max}}\int\int_{S_k w+v}\{\Psi(x, y, z, \xi, \eta, c_k)\\ &\times[\Delta\phi_\xi(\xi, \eta, c_k + 0) - \Delta\phi_\xi(\xi, \eta, c_k - 0)]\\ &- \Psi_\zeta(x, y, z, \xi, \eta, c_k)[\Delta\phi(\xi, \eta, c_k + 0)\\ &- \Delta\phi(\xi, \eta, c_k - 0)]\}\, d\xi\, d\eta\\ &+ \frac{1}{4\pi}\int\int\int_V \Psi_\xi(x, y, z, \xi, \eta, \zeta)\\ &\times\left\{\frac{1}{2}[(\phi')_\xi + \Delta\phi_\xi]^2 - \frac{1}{2}(\phi')_\xi^2\right\} d\xi\, d\eta\, d\zeta \end{aligned} \quad (10)$$

where

$$\Psi(x, y, z, \xi, \eta, \zeta) = \frac{1}{\sqrt{(x - \xi)^2 + (y - \eta)^2 + (z - \zeta)^2}}$$

The domain of integration is shown in Fig. 1. The control volume is indicated by C in Fig. 1, which is an infinitesimal radius sphere whose center is $P(x, y, z)$. To maintain the mathematical correctness of the formulation, the domain is carefully defined where $\Delta\phi$ should be C^1 continuous. The domain is bounded by the following four areas: 1) lower and upper surfaces of $S_k w + v$, which indicates the mean plane of wing-k and its wake; 2) both sides of shock waves, which are assumed to be nearly perpendicular to the wing surface; 3) the infinite far-field boundary; and 4) the infinite outflow boundary. At the infinite far-field and outflow boundaries, the small disturbance associating wings' geometry should be trifling so that we can assume $\Delta\phi$ and the velocity change (the derivative of $\Delta\phi$) to be zero. The contribution of the surface integrals over the infinite boundaries vanishes. Furthermore, the contribution of the integrals along the shock surface vanishes because of the shock-polar conditions.[14] The triple integral in Eq. (10) should be evaluated by using the finite part integration as mentioned in Ref. 4 to exclude $P(x, y, z)$, where Ψ becomes singular, from the domain of integral.

To combine Eq. (10) with the other equations, Eqs. (8) and (9), further calculus is needed because Eqs. (8) and (9) are the functions of x and z derivatives of $\Delta\phi$. In detail, for wing-k, we differentiate both sides of Eq. (10) with respect to x and

add the resulting equation of $\Delta\phi_x(x, y, z)$ at $z = c_k + 0$ to that at $z = c_k - 0$. A simultaneous k_{max} integral equation system:

$$\Delta us_k(x, y) = -\frac{1}{2\pi}\int\int_{S_k w} \Psi_x(x, y, c_k, \quad \xi, \eta, c_k) \times \Delta ws_k(\xi, \eta)\, d\xi\, d\eta + \chi s_k(x, y) - \frac{1}{2\pi}\sum_{p\neq k}\int\int_{S_k w} [\Psi_x(x, y, c_k, \quad \xi, \eta, c_p) \times \Delta ws_p(\xi, \eta) - \Psi_\zeta(x, y, c_k, \quad \xi, \eta, c_p) \times \Delta ua_p(\xi, \eta)]\, d\xi\, d\eta + \frac{1}{4\pi}\int\int\int_V \Psi_{\xi x}(x, y, 0, \quad \xi, \eta, \zeta) \times [\chi(\xi, \eta, c_k + \zeta) + \chi(\xi, \eta, c_k - \zeta)]\, d\xi\, d\eta\, d\zeta \tag{11}$$

where

$$\chi s_k(x, y) = \chi(x, y, c_k + 0) + \chi(x, y, c_k - 0)$$

is obtained. Next, we differentiate both sides of Eq. (10) with respect to z, and add the equation of $\Delta\phi_z(x, y, z)$ at $z = c_k + 0$ to that at $z = c_k - 0$. Performing an integration by parts on the sum leads to k_{max} integral equations as

$$\Delta wa_k(x, y) = \frac{1}{2\pi}\int\int_{S_k w}\left(\frac{\Delta ua_k(\xi, \eta)}{(y - \eta)^2} \times \left\{1 + \frac{x - \xi}{[(x - \xi)^2 + (y - \eta)^2]^{1/2}}\right\}\right) d\eta\, d\xi + \frac{1}{2\pi}\sum_{p\neq k}\int\int_{S_p w}\left(\frac{\Delta ua_p(\xi, \eta)}{(y - \eta)^2 + \bar{c}_{kp}^2} \times \left\{1 + \frac{x - \xi}{[(x - \xi)^2 + (y - \eta)^2 + \bar{c}_{kp}^2]^{1/2}}\right\}\right) d\xi\, d\eta - \frac{1}{2\pi}\sum_{p\neq k}\int\int_{S_p w} \Psi_z(x, y, c_k, \quad \xi, \eta, c_p) \times \Delta ws_p(\xi, \eta)\, d\xi\, d\eta\, d\zeta - \frac{1}{2\pi}\sum_{p\neq k}\int\int_{S_p w} \Delta ua_p(\xi, \eta) \times \frac{\bar{c}_{kp}^2}{[(y - \eta)^2 + \bar{c}_{kp}^2]^2}\cdot(2 + 3q - q^3)\, d\xi\, d\eta + \frac{1}{4\pi}\int\int\int_V \Psi_{\xi z}(x, y, 0, \quad \xi, \eta, \zeta)\cdot[\chi(\xi, \eta, c_k + \zeta) - \chi(\xi, \eta, c_k - \zeta)]\, d\xi\, d\eta\, d\zeta \tag{12}$$

where

$$q = \frac{x - \xi}{\sqrt{(x - \xi)^2 + (y - \eta)^2 + \bar{c}_{kp}^2}}, \qquad \bar{c}_{kp} = c_k - c_p$$

The following functions are implied in Eqs. (11) and (12):

$$\Delta ws_k(x, y) = \Delta\phi_z(x, y, c_k + 0) - \Delta\phi_z(x, y, c_k - 0) = \frac{\partial}{\partial x}[\Delta f_{k+}(x, y) - \Delta f_{k-}(x, y)] \tag{13}$$

$$\Delta wa_k(x, y) = \Delta\phi_z(x, y, c_k + 0) + \Delta\phi_z(x, y, c_k - 0) = \frac{\partial}{\partial x}[\Delta f_{k+}(x, y) + \Delta f_{k-}(x, y)] \tag{14}$$

$$\Delta us_k(x, y) = \Delta\phi_x(x, y, c_k + 0) + \Delta\phi_x(x, y, c_k - 0) = -\frac{K}{2\beta^2}(\Delta Cp_{k+} + \Delta Cp_{k-}) \tag{15}$$

$$\Delta ua_k(x, y) = \Delta\phi_x(x, y, c_k + 0) - \Delta\phi_x(x, y, c_k - 0) = -\frac{K}{2\beta^2}(\Delta Cp_{k+} - \Delta Cp_{k-}) \tag{16}$$

Through the previous process, surface integrals over the upper and lower side of the wake of each wing are canceled. Thus the surface integral over wings' surface Sw remains.

For an inverse problem, the unknowns of Eq. (11) are Δws_k ($k = 1, 2, \ldots, k_{max}$), which represent the symmetric part of geometric correction and, in other words, correction in thickness. The unknowns of Eq. (12), Δwa_k ($k = 1, 2, \ldots, k_{max}$), are representing the antisymmetric part of geometrical correction, which is curvature change of the camber of each wing section. Considering multiple wings in a flowfield, the resulting equations have more terms and complexity than equations for a single wing system. The second, third, and fourth terms of Eq. (12) as well as the second term of Eq. (11) appear to take in the mutual interaction among wings and allow any arbitrary z location of each wing. For single-wing cases, the z location of a wing is always zero.

In addition, to evaluate the triple integrals of Eqs. (11) and (12) an assumption is introduced concerning $\chi(x, y, z)$. We know $\chi_k(x, y, z)$ only over each wing surface boundary, nevertheless, triple integrals require the knowledge of $\chi(x, y, z)$ all over the domain. The assumption is that the $\chi(x, y, z)$ is a linear combination of χ_k ($k = 1, 2, \ldots, k_{max}$), which is expressed as

$$\chi_k(x, y, z) = \chi_k(x, y, +0)\exp[-2R_{k+}(x, y)(z - c_k)] \quad \text{for} \quad z \geq c_k \tag{17}$$

$$\chi_k(x, y, z) = \chi_k(x, y, -0)\exp[+2R_{k-}(x, y)(z - c_k)] \quad \text{for} \quad z < c_k \tag{18}$$

where

$$R_{k\pm}(x, y) = \text{abs}\left[\frac{\partial^2}{\partial x^2} f_{k\pm}(x, y)/\phi_x(x, y, c_k \pm 0)\right] \tag{19}$$

Equations (17–19) come from the assumption employed in Ref. 4 to approximate the ϕ_x profile along z. $\chi_k(x, y, z)$ represents the nonlinear term of the transonic small disturbance equation associating with wing-k. $\chi_k(x, y, \pm 0)$ is its value on the wing surface:

$$\chi_k(x, y, \pm 0) = \frac{1}{2}[(\phi_x^I + \Delta\phi_x)^2 - (\phi_x^I)^2] = -\frac{K^2}{8\beta^4}[(Cp_{k\pm}^T)^2 - (Cp_{k\pm}^I)^2] \tag{20}$$

$\chi_k(x, y, \pm 0)$ has an effective value only if it is on the upper or lower surface of wing-k, otherwise $\chi_k = 0$. Therefore, the triple integral term of Eq. (11) yields to

$$\frac{1}{2\pi}\sum_{p=1}^{k_{max}}\left\{\int\int_{S_p w}\chi_p(\xi, \eta, +0)\int_0^\infty \Psi_{\xi x}(x, y, 0, \quad \xi, \eta, \zeta - \bar{c}_{kp}) \times \exp[-2R_+(\xi, \eta)\zeta]\, d\zeta\, d\eta\, d\xi + \int\int_{S_p w}\chi_p(\xi, \eta, -0) \times \int_0^\infty \Psi_{\xi x}(x, y, 0, \quad \xi, \eta, \zeta + \bar{c}_{kp}) \times \exp[-2R_-(\xi, \eta)\zeta]\, d\zeta\, d\eta\, d\xi\right\} \tag{21}$$

To assure the uniqueness of the solution to integral Eq. (11), a constraint has to be imposed on the unknown function Δws_k. The closure condition at the trailing edge that was previously used in Ref. 4 is adopted:

$$\int_{\text{Leading Edge}}^{\text{Trailing Edge}} \Delta ws_k(x, y)\, dx = 0 \qquad (k = 1, 2, \ldots, k_{max}) \tag{22}$$

III. Piecewise Functions and Discretization

To enhance the applicability of the method, several aerodynamic properties are assumed to be piecewise linear/constant. Equations (15) and (16) are transformed into discretized equations that can be solved numerically. Each wing surface is divided into panels as shown in Fig. 2. The wing-k has $2J(k) + 1$ panels in the spanwise (y) direction and $I(k)$ panels in the chordwise (x) direction. The coordinate (x^j_i, y^j) denotes the center of the panel (i, j). The panel (i, j) spreads from $x^j_{i-1/2}$ to $x^j_{i+1/2}$ along x direction and from $y^{j-1/2}$ to $y^{j+1/2}$ along y direction. Inside each panel, Δus_k, Δua_k, χs_k, $\chi_k(x, y, \pm 0)$, $R_{k\pm}$, and Δwa_k are assumed to be constant. Δws_k is assumed to vary linearly along x, but to be constant along y. Therefore, Eq. (15) for Δws_k yields to

$$\begin{aligned}\Delta us_k(x^j_i, y_j) = &\sum_{l=1}^{I(k)+1}\sum_{m=0}^{J(k)} \mu^{s_k}_{i,j,l,m}\Delta ws_k(x^m_{l-1/2}, y_m)\\ &+ \sum_{l=1}^{I(k)}\sum_{m=0}^{J(k)} (\nu^{s_k}_{i,j,l,m} + \tilde{\nu}^{s_k}_{i,j,l,m}) + \chi s_k(x^j_i, y_j)\\ &+ \sum_{p\neq k}\sum_{l=1}^{I(p)+1}\sum_{m=0}^{J(p)} \mu^{s_p}_{i,j,l,m}\Delta ws_p(x^m_{l-1/2}, y_m)\\ &+ \sum_{p\neq k}\sum_{l=1}^{I(p)}\sum_{m=0}^{J(p)} \kappa^{s_p}_{i,j,l,m}\Delta ua_p(x^m_l, y_m)\\ &+ \sum_{p\neq k}\sum_{l=1}^{I(p)}\sum_{m=0}^{J(p)} (\nu^{s_p}_{i,j,l,m} + \tilde{\nu}^{s_p}_{i,j,l,m}) \qquad (23)\end{aligned}$$

considering the symmetry of the wings' planform and flowfield with respect to $y = 0$.

The constraint for each wing section expressed in Eq. (22) yields to

$$\sum_{l=1}^{I(k)} \frac{1}{2}\left[\Delta ws_k(x^j_{i-1/2}, y_j) + \Delta ws_k(x^j_{i+1/2}, y_j)\right]\cdot(x^j_{i-1/2} - x^j_{i+1/2}) = 0 \qquad (24)$$

(for each j: $j = 0, 1, 2, \ldots, J(k)$ of each k: $k = 1, 2, \ldots, k_{max}$).

Because of the piecewise function approximation stated earlier, the center of each panel is used to express the piecewise constant functions such as Δus_k, etc. The number of such points is $I(k)$ along the chordwise direction at each span station. On the other hand, Δws_k is defined at the midpoint of every side parallel to the x axis of panels. $I(k) + 1$ points are used to express the function Δws_k at each span station. Equation (23) provides $I(k)$ equations and Eq. (24) does one equation. Consequently, we have $I(k) + 1$ linear equations for $I(k) + 1$ unknowns expressed as $\Delta ws_k(x^j_{i+1/2}, y^j)$ at each span station. That guarantees the existence and the uniqueness of the solution of the discretized equation system.

Equation (16) for Δwa_k yields to

$$\begin{aligned}\Delta wa_k(x^j_i, y_j) = &\sum_{l=1}^{I(k)}\sum_{m=0}^{J(k)} \mu^{a_k}_{i,j,l,m}\Delta ua_k(x^m_l, y_m)\\ &+ \sum_{l=1}^{I(k)}\sum_{m=0}^{J(k)} (\nu^{a_k}_{i,j,l,m} - \tilde{\nu}^{a_k}_{i,j,l,m}) + \sum_{p\neq k}\sum_{l=1}^{I(p)}\sum_{m=0}^{J(p)} \mu^{a_p}_{i,j,l,m}\Delta ua_p(x^m_l, y_m)\\ &+ \sum_{p\neq k}\sum_{l=1}^{I(p)+1}\sum_{m=0}^{J(p)} \kappa^{a_p}_{i,j,l,m}\Delta ws_p(x^m_{l-1/2}, y_m)\\ &- \sum_{p\neq k}\sum_{l=1}^{I(p)}\sum_{m=0}^{J(p)} \tau^{a_p}_{i,j,l,m}\Delta ua_p(x^m_l, y_m)\\ &+ \sum_{p\neq k}\sum_{l=1}^{I(p)}\sum_{m=0}^{J(p)} (\nu^{a_p}_{i,j,l,m} - \tilde{\nu}^{a_p}_{i,j,l,m}) \qquad (25)\end{aligned}$$

The coefficients that appear in Eqs. (23) and (25), $\mu^s_{i,j,l,m}$, etc., are the piecewise integrals over each panel. All of the piecewise integrals can be treated analytically. Their integral representations are shown in detail in Ref. 16. The evaluation of the right-hand side of Eq. (23) determines the x derivative of the antisymmetric part of the geometric correction of each section contour Δwa_k directly. For the x derivative of the symmetric part Δws_k, a system of $\Sigma_k [I(k) + 1][J(k) + 1]$ ($k = 1, \ldots, k_{max}$) linear equations should be solved. Therefore, the geometric correction of each wing Δf_k is solved by integrating Δws_k and Δwa_k with respect to x.

IV. Design Procedure

The inverse problem solver based on the new formulation is incorporated into a design loop presented in Fig. 3. The

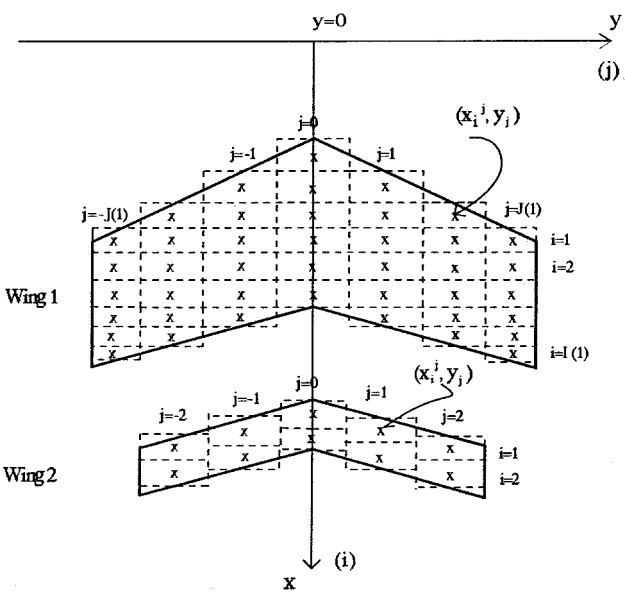

Fig. 2 Panels on integral surface.

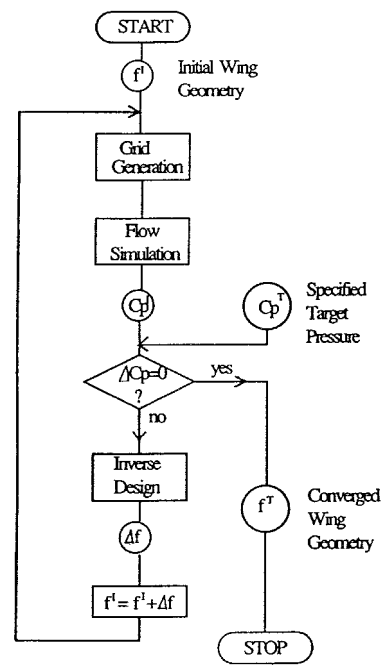

Fig. 3 Design procedure.

design procedure is an iterative residual correction method[4] that starts with an initial guess of geometry of wings. Then it conducts flow simulation and inverse design in turn until the residual becomes negligibly small. The flow simulation consisting of a grid generation and a flow solver gets the residual ΔCp. The inverse design solves an inverse problem to obtain the geometrical correction Δf to design the wings' section contours. Any kind of flowfield, from a potential flow to a Navier–Stokes flow, can be treated with this procedure since the flow solver and the inverse design part are independent of each other. Here, the inverse design is coupled with Reynolds-averaged Navier–Stokes flow simulation so that viscous effect can be taken into consideration for the design. We generate grid points all over the space about wings at each iteration of the design process. The numerical algorithms to obtain the steady state of a flowfield are the LU decomposed alternating direction implicit (LU–ADI) method for time integration with the local time stepping and the total variation diminishing type upwind finite differencing in space using the MUSCL interpolation and Roe's Riemann solver. The turbulent viscosity is evaluated by the Baldwin–Lomax model.

After every inverse design step, we smooth the wing geometry f to moderate geometrical oscillations as follows. $f_{k\pm}(x)$ at each span station of each wing is modified to be on the curve expressed as

$$f_{\pm}(x^*) = c_{0\pm}\sqrt{x^*} + \sum_{n=1}^{7} c_{n\pm}(x^*)^n \qquad (26)$$

where

$$x^* = x - x_{\text{Leading Edge}}$$

We employ the least-square approximation curve-fitting algorithm. The algorithm calculates the coefficients $C_{0\pm}$ and $C_{n\pm}$.

V. Results of Design Problems

Several examples of two airfoil systems are preliminary designed by the present method. The primary object of this paper is to show the feasibility of the new formulation. The authors think that the design of airfoil systems adequately perform to inspect the feasibility since airfoil design is the simple example of design of wings. For the case of two airfoils, two long span wings are put in a flowfield when the inverse problem is solved, because it is formulated in three-dimensional space. We specify the three-dimensional pressure distribution over the wings as the target pressure. In this way, Hirose et al.[17] designed a single airfoil successfully by using Takanashi's method. If there is anything wrong with the formulation of the inverse problem and implementation of the solver, the inverse design does not work for airfoil design. Thus, we examine airfoil cases here because of their simplicity to inspect the results and efficiency of the Navier–Stokes flow simulation.

The initial geometry of each example is shown in Fig. 4 as the dashed contours. Every section has a NACA 0012 airfoil shape with 0-deg angle of attack. Example 1 is regarded as a tandem system. Both airfoils' chord lengths are 1.0, and the x distance (Δx) and z distance (Δz) from the trailing edge of the front airfoil to the leading edge of the rear airfoil are 1.0 and 0.05, respectively. Example 2 can be considered as a simplified system of a multicomponent system, a main part and a flap. The chord length of the main part is 1.0, whereas that of the flap is 0.35, and Δx and Δz are 0.1 and 0.01, respectively. The CPU time required is 16.5 s on a 1.7-GFlop vector computer to solve a two-wing inverse problem, when the total number of panels $I(1)\cdot[J(1) + 1] + I(2)\cdot[J(2) + 1]$ is 300. The required memory is less than 10 Mbytes. $I(k)$, the number of panels in the chordwise direction, is 50, for the design explained in the following sections.

A. Redesign of Known Shape

First of all, we examine the method by designing the known shape, which is the tandem of two RAE2822 airfoils. The specified target pressure distribution is obtained by the Navier–Stokes simulation of flow about two RAE2822 airfoils whose positions are the same as those of Example 1 (Fig. 4) except Δz (=0.087), and both airfoils have an angle of attack of 2.5 deg. Figure 5 shows the initial and converged states. At the initial stage both airfoils are NACA 0012 shape with the angle of attack of 0 deg. The freestream Mach number M_∞ is 0.60 and the Reynolds number is 1×10^6. It needs five iterations of the design loop to converge. At the converged stage the agreement between the target and computed pressure distributions around the leading edge is poorer than that of the rest region. The two reasons explain the poor agreement. First, the small disturbance approximation deteriorates in the vicinity of the stagnation point, i.e., the leading edge of the airfoil. The other is that the size of panels is not sufficiently fine there. In fact, when we prepare doubled fine panel distribution (100 panels) in the chordwise direction, the agreement there be-

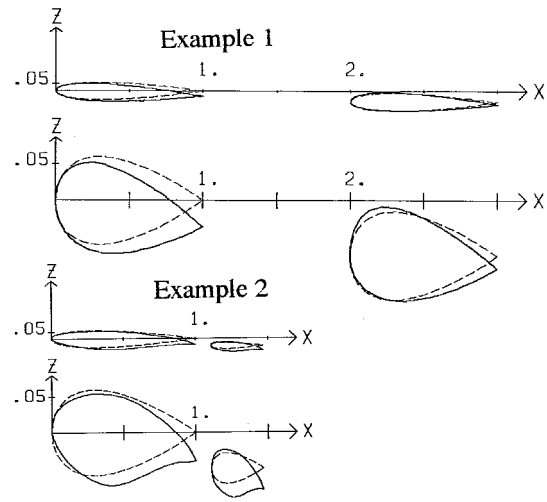

Fig. 4 Initial (dashed line) and designed (solid line) contours in real scale and magnified five times in z.

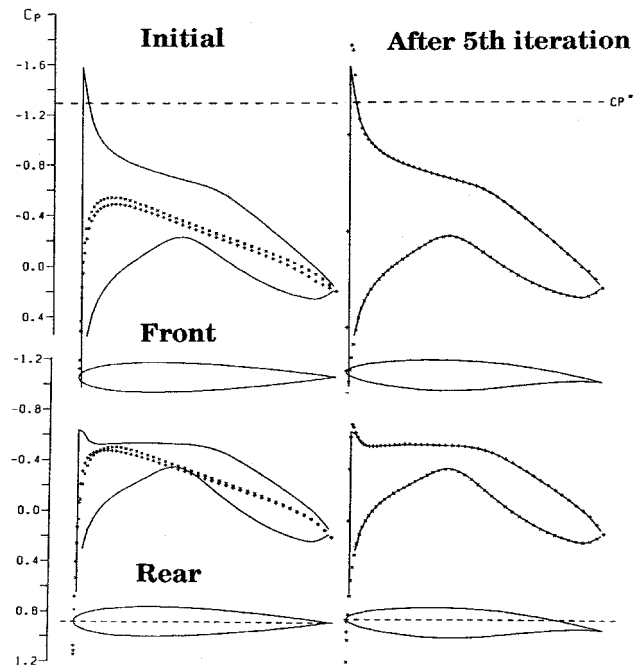

Fig. 5 History of redesigning ($M_\infty = 0.6$, $Re = 1 \times 10^6$).

comes much better at the converged stage. In addition, the number of iterations to reach the convergence is reduced with the finer panel distribution. The designed shape is compared with the target shape in Fig. 6. The new method works quite well on redesigning. Little discrepancy between the two shapes is observed.

B. Design of Arbitrary Shape

Figure 7 displays the convergence history of the design process on Example 1 (see Fig. 4). M_∞ is 0.73 and the Reynolds number is 1×10^6. We specify the pressure distribution of solid lines in the figure as the target, which is obtained by Navier–Stokes flow simulation around two arbitrarily inclined NACA 0012 airfoils with M_∞ of 0.76. The target pressure of the front wing has a strong shock that makes it difficult to solve the inverse problem. In the vicinity of a sharp shock wave, the nonlinear term of the small disturbance equation takes a relatively major part, and deteriorates the accuracy of the formulation of the inverse problem, because the formulation is essentially in the first order. This is one examination to assure the robustness of the inverse problem solver, whereas the pressure distribution is not very desirable for a realistic design target. In fact, a pressure distribution with strong shock waves should not be specified as a target pressure distribution, because strong shock waves cause large drag force. Fortunately, the flow is not largely separated.

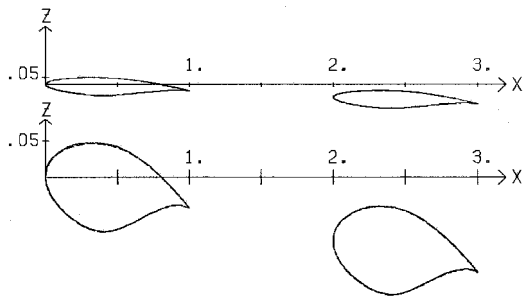

Fig. 6 Comparison of target (dashed line) and designed (solid line) contours.

In Fig. 7, the leftmost plot shows the initial pressure distribution and geometry contour of each airfoil. From left to right are presented pressure distributions and corresponding geometry contours after one, three, and five iteration(s) of the design loop. The current pressure distribution is plotted with symbols. The symbol + indicates the upper surface pressure and × designates the lower surface pressure. At the initial stage, both airfoils have negative lift in spite of their symmetrical shapes with 0-deg angle of attack. This implies the slight interaction between two airfoils. We obtain the wing geometry that almost realizes the target pressure distribution after five iterations of the design loop. In the vicinity of the shock wave, the complete agreement with the target pressure is not always attainable. The further iteration of the loop or the finer panel discretization does not improve the designed result in the vicinity of the shock wave. Sophisticated strategy should be taken for the improvement. Reference 10 mentioned some of the strategy such as modification of the equation and smoothing of the wing surfaces.

Figure 8 presents the convergence history of Example 2 (see Fig. 4). M_∞ is 0.60 and the Reynolds number is 1×10^6. The specified target pressures drawn with solid lines are those used for redesigning a known shape. In Fig. 8, the leftmost plot shows the initial pressure distribution and geometry contour of each airfoil. From left to right are presented pressure distributions and corresponding geometry contours after one, five,

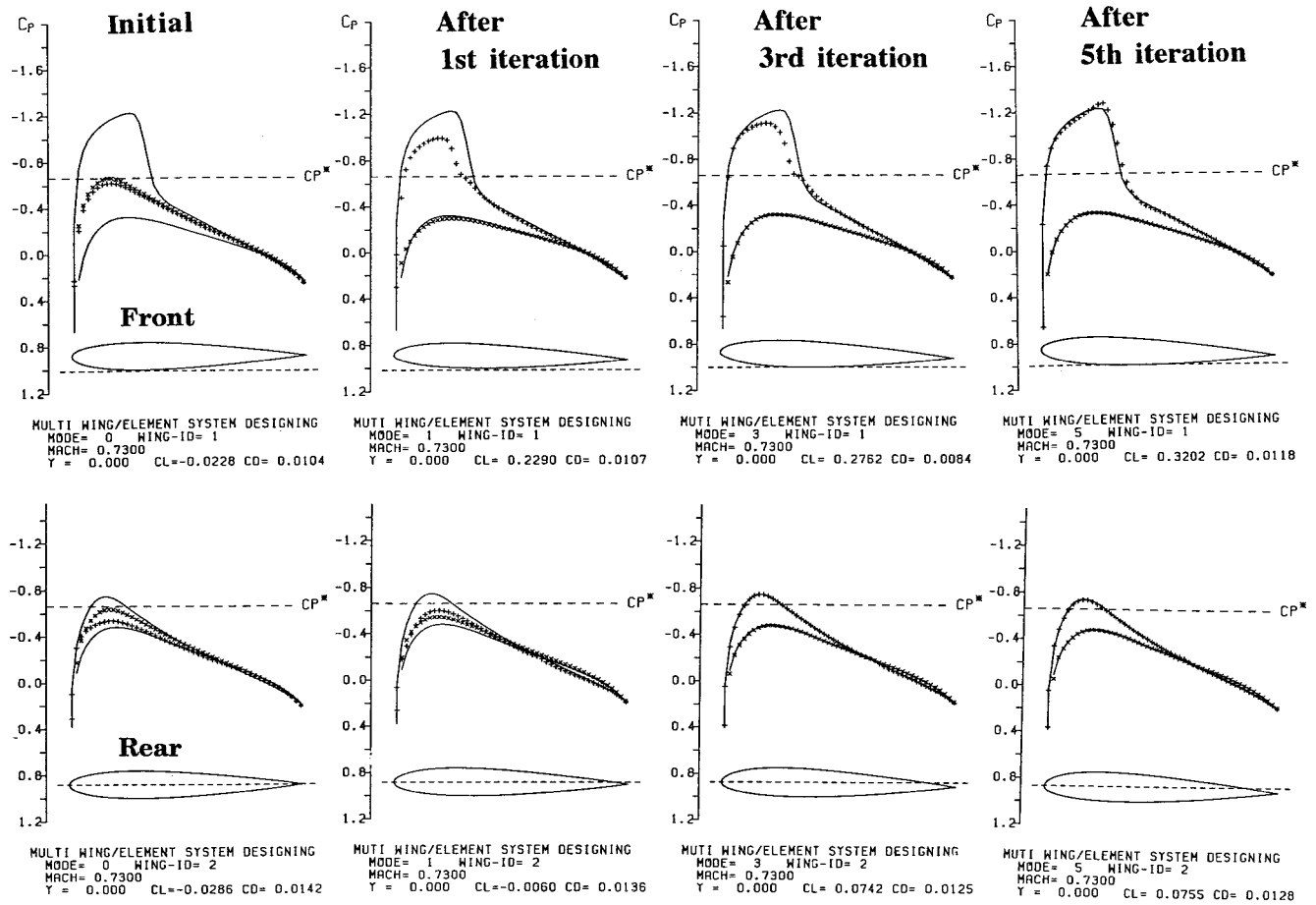

Fig. 7 Design process history on Example 1 ($M_\infty = 0.73$, $Re = 1 \times 10^6$). Target *Cp*, ——; current *Cp*, + and ×.

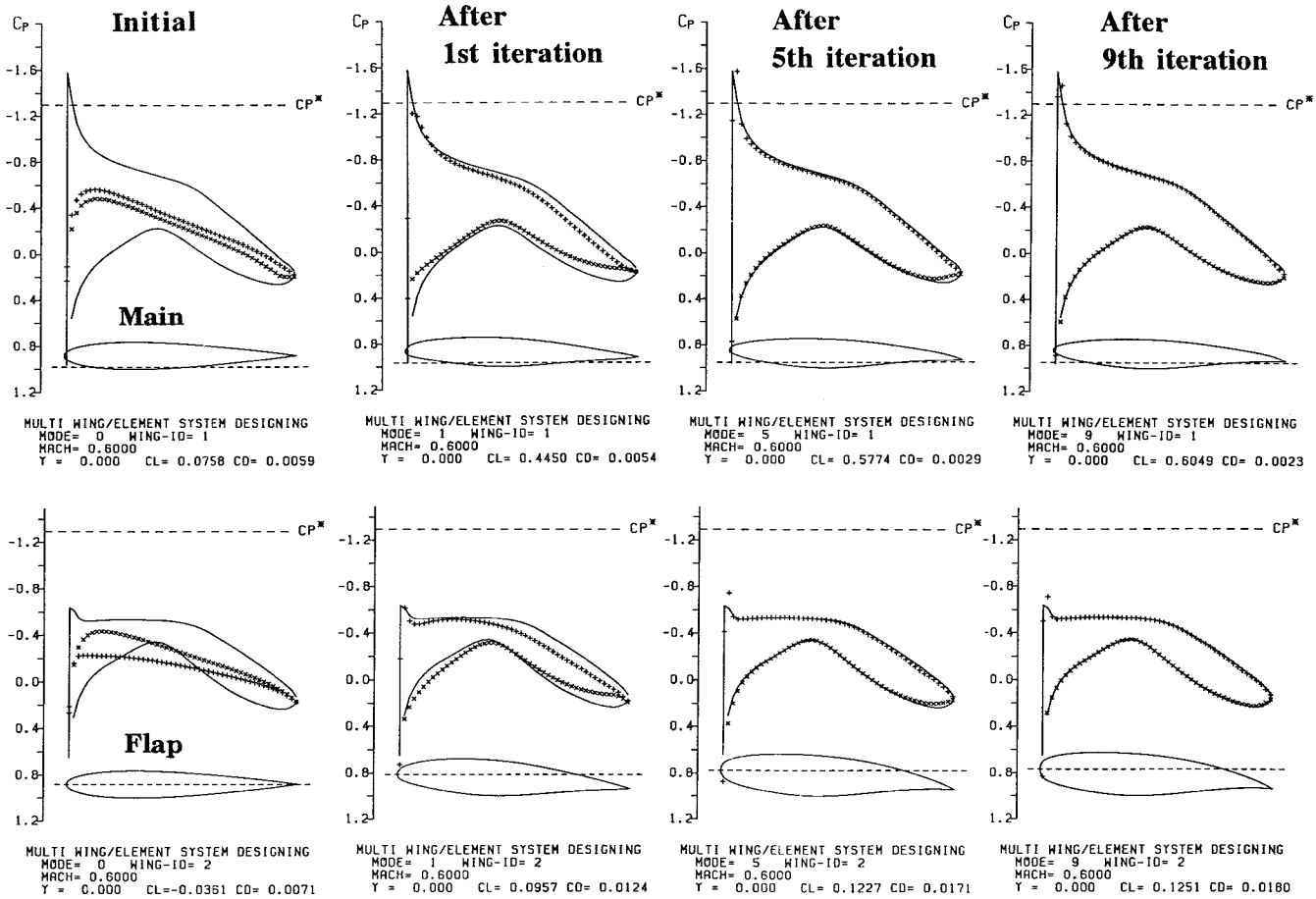

Fig. 8 Design process history on Example 2 ($M_\infty = 0.60$, $Re = 1 \times 10^6$). Target Cp, ——; current Cp, + and ×.

and nine iteration(s) of the design loop. At initial stage, the lift of the main part is slightly positive, and that of the flap is definitely negative. This fact suggests that there is strong aerodynamic interaction between two airfoils. We obtain the designed geometry after nine iterations. As stated before, the doubled fine panel discretization improves the agreement between the target and the calculated pressures of the convergence state as well as reduces the number of iterations required for convergence by 20%.

The comparison is made in Fig. 4 between the initial and designed geometry of Example 1 and Example 2. Figure 4 shows the airfoil contours in the real scale and in the magnified scale in the z direction. Both airfoils of Example 1 have assumed the same angle of attack, as expected. On the other hand, both airfoils of Example 2 have changed greatly their shapes and angles of attack. The flap-like airfoil has definitely thickened and inclined. It is interesting to compare the designed shape of Example 2 with that of the redesigning problem, both of which we specify the same target pressure distribution. It can be seen that difference in the interaction between airfoils precisely affects designed shapes. Designed shapes of both problems differ greatly in three points: 1) the shape of the trailing edge of a front airfoil, 2) the angle of attack of a rear airfoil, and 3) the thickness of a rear airfoil.

VI. Concluding Remarks

An inverse design method for multiple wing systems has been devised on the basis of Takanashi's method. The new method determines wing section geometry that realizes the specified target pressure distribution over wings. It designs multiple wings in a transonic/high-subsonic flowfield simultaneously. The inverse problem is formulated to be integral equations that relates geometrical correction to pressure difference. The formulation starts from the transonic small disturbance equation and considers interacting effects among wings. The inverse problem is solved numerically with discretizing wings' surface into small panels. An iterative design procedure is constructed coupling the new inverse problem solver and a Navier–Stokes flow analysis code. The procedure has been applied to preliminary design problems to show the feasibility of the new inverse design method. The authors confirm that the method works well for the design of airfoil shapes of multiple airfoil systems.

Through the research we have also found the following facts:

1) The inverse problem can be formulated analytically for a flowfield of multiple wings interacting with each other.

2) The inverse design method is able to evaluate interacting effect among wings accurately and provide design results relevant to the effect.

3) The method is so efficient in computational time and memory that it is a promising concept for more complicated design problems.

References

[1]Laburujere, T. E., and Slooff, J. W., "Computational Methods for the Aerodynamic Design of Aircraft Components," *Annual Review of Fluid Mechanics*, Vol. 25, 1993, pp. 183–214.

[2]Dulikravich, G. S., "Shape Inverse Design and Optimization for Three-Dimensional Aerodynamics," AIAA Paper 95-0695, Jan. 1995.

[3]Campbell, L. R., "Efficient Constrained Design Using Navier-Stokes Codes," AIAA Paper 95-1808, June 1995.

[4]Takanashi, S., "Iterative Three-Dimensional Transonic Wing Design Using Integral Equations," *Journal of Aircraft*, Vol. 22, No. 8, 1985, pp. 655–660.

[5]Fujii, K., and Takanashi, S., "Aerodynamic Aircraft Design Meth-

ods and Their Notable Applications," *International Conference on Inverse Design Concepts and Optimization in Engineering Sciences*, ICIDSE-III, 1991, pp. 31–45.

[6]Xia, Z. X., Zhu, Z. Q., and Vu, L. Y., "A Computational Method for Inverse Design of Transonic Airfoil and Wing," AIAA Paper 93-3482, Aug. 1993.

[7]Lorentzen, L., "Development of Inverse Airfoil Design for Transonic Applications," Federal Aviation Administration, TN 1993-37, Oct. 1993.

[8]Hua, J., Yang, Q. Z., Xi, D. K., Zhang, Z. Y., Fu, D. W., Zhang, Z. L., and Wang, L., "Design and Experimental Investigation of Transonic Natural Laminar Flow Wings," International Council of the Aeronautical Sciences, 94-4,7,3, Sept. 1994.

[9]Obayashi, S., and Takanashi, S., "Genetic Optimization of Target Pressure Distributions for Inverse Design Methods," AIAA Paper 95-1649, June 1995.

[10]Bartelheimer, W., "An Improved Integral Equation Method for the Design of Transonic Airfoils and Wings," AIAA Paper 95-1688, June 1995.

[11]Ormsbee, I. A., and Chen, W. A., "Multiple Element Airfoil Optimized for Maximum Lift Coefficient," *AIAA Journal*, Vol. 10, No. 12, 1972, pp. 1620–1624.

[12]Narramore, J. C., and Beaty, T. D., "An Inverse Method for Multielement High-Lift Systems," AIAA Paper 75-879, June 1975.

[13]Shigemi, M., "A Solution of Inverse Problems for Multi-Element Aerofoils through Application of Panel Method," *Transactions of the Japan Society for Aeronautical and Space Sciences*, Vol. 28, No. 80, 1985, pp. 97–107.

[14]Drela, M., "Design and Optimization Method for Multi-Element Airfoils," AIAA Paper 93-0969, Feb. 1993.

[15]Heaslet, M. A., and Spreiter, J. R., "Three Dimensional Transonic Flow Theory Applied to Slender Wings and Bodies," NACA 1318, 1957.

[16]Matsushima, K., and Takanashi, S., "An Inverse Design Methods for Transonic Multiple Wing Systems on Integral Equations," AIAA Paper 96-2465, June 1996.

[17]Hirose, N., Takanashi, S., and Kawai, N., "Transonic Airfoil Design Based on Navier-Stokes Equation to Attain Arbitrarily Specified Pressure Distribution—An Iterative Procedure," AIAA Paper 85-1592, July 1985.